Measurement of radiated noise from surface ships – Influence of the sea surface reflection coefficient on the Lloyd's mirror effect

Christian Audoly and Valentin Meyer

DCNS Research, Toulon, France

ABSTRACT

The assessment of ship underwater noise signature is highly important not only to a range of naval applications but for the assessment and mitigation of shipping related noise impact on marine animals. One of the main phenomena affecting ship radiated noise measurement is Lloyd's mirror effect, which describes the interference between the direct sound path and the path reflected on sea surface. Having published a first standard for radiated noise measurement in deep waters for comparison purposes, the ISO committee on underwater acoustics is working towards an objective of correcting the Lloyd's mirror effect. While it is assumed that the surface of the ocean acts as a perfect mirror, this is not often the case due to sea surface deformation. The aim of the present study is to investigate the influence of a non-perfect reflection coefficient on the Lloyd's mirror effect. This is achieved through the use of different models taken from the literature that provide an effective reflection coefficient depending on frequency, grazing angle and sea state. Results are presented in the form of acoustic pressure maps at short propagation distances and of frequency responses at different observation points, for sea states up to 3. Simulations show that the effect is small at low frequencies, and at high frequencies a deviation of up to 3 dB appears. However, these results are dependent on the reflection coefficient model used.

1 INTRODUCTION

The reduction of ship underwater radiated noise has been an important objective of Navies for several decades, in order to reduce the risk of detection by adverse passive sonar from a few categories of vessels, such as frigates. Demanding regulations have been proposed to limit noise radiated from fishery research vessels (*Underwater noise of research vessels*, 1995). Indeed, recently built vessels of that type are much more silent (Nejedl, 2012). Regarding commercial ships, due to the steady increase of maritime traffic, there is a growing concern amongst the scientific community regarding the environmental impact of the related underwater noise and its consequences on marine life. Currently, there are no regulations addressing this issue except some non-mandatory guidelines (*Guidelines for the reduction of underwater noise*, 2014). However, there have been some actions implemented at international level, such as the ECHO Program (Knight, 2017) and the validation of a methodology in the scope of the European Project AQUO (Audoly, 2017).

In that context, it is important to define reliable procedures for the measurement of underwater radiated noise from ships. In the scope of the ISO committee on underwater acoustics, the 17208-1 standard was published, describing a method for ship radiated measurement applicable in deep water which was derived from grades A and B of American standard ANSI-ASA S12.64/Part1:2009. The ISO standard is a precision method for comparison purposes, giving a measurement of radiated noise affected by the reflection of waves on the sea surface, i.e. the Lloyd's mirror effect presented in section 2.

The computation of underwater noise maps addressing the impact on marine life requires the representation of each vessel in the form of an equivalent omnidirectional point source of level SL that would produce the same pressure field. Therefore the affected radiated noise level must be corrected from the Lloyd's mirror effect. The ISO standardization committee is currently working on this issue.

It should be noted that when dealing with the Lloyd's mirror effect, it is generally assumed that the sea surface is perfectly flat (Ainslie, 2010), leading to a theoretical reflection coefficient of amplitude one, with a 180° phase shift. In reality however, this is seldom the case because of the presence of waves or roughness in relation with sea state, wind speed and other environmental parameters. After a reminder of the basics of the Lloyd's mirror effect, and a review of models for reflection coefficient of sea surface (section 3), the purpose of the present paper is to study the effect of a non-perfect reflection on the Lloyd's mirror effect in relation with the ship radiated noise measurement procedures (section 4).

2 THE LLOYD'S MIRROR EFFECT AND ITS CONSEQUENCE ON SHIP RADIATED NOISE MEASUREMENT

For simplicity, we shall assume that the environment is deep waters (i.e. the interaction of waves with sea bottom is not taken into account) and that the sea water speed of sound c is constant in the water column and invariant with distance. In that case, modelling of underwater acoustic propagation can be done simply by using a ray tracing approach. Underwater radiated noise emission from a surface ship occurs a few meters below sea surface, denoted by the quantity d. Therefore, when observing the sound pressure level (SPL) at a given observation point located at depth z_M and range D_M, there is an interference between the direct propagation path and the path reflected on sea surface, known as the Lloyd's mirror effect (Figure 1).

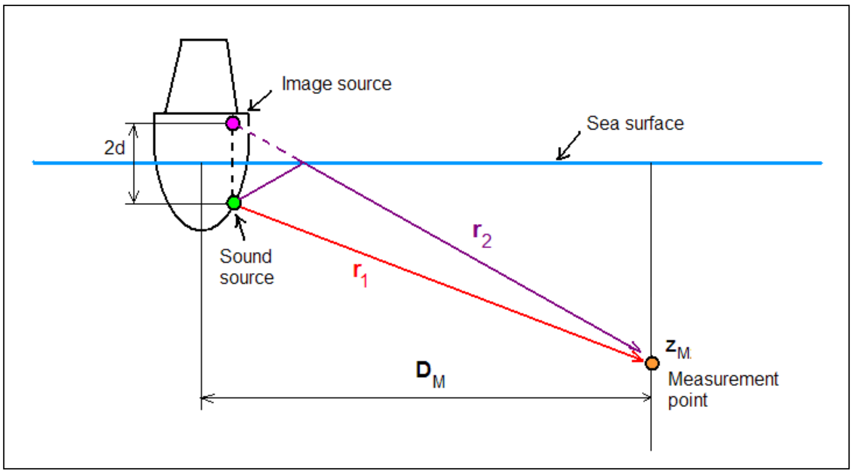

Figure 1: The Lloyd's mirror effect in relation with ship radiated noise.

At a given single frequency f in an unbounded domain, the SPL would correspond to spherical spreading only and would depend only on the distance $r_1 = \sqrt{D_M^2 + (z_M - d)^2}$:

$$SPL_{direct} = 20logS + 20log\left|\frac{exp(-ikr_1)}{r_1}\right| \quad (1)$$

where S is acoustic source strength, and $k = \frac{2\pi f}{c}$ is the wavenumber.

In presence of the sea surface, characterized by the reflection coefficient R, which depends on the grazing angle θ, the total SPL is given by:

$$SPL_{total} = 20logS + 20log\left|\frac{exp(-ikr_1)}{r_1} + R(f,\theta)\frac{exp(-ikr_2)}{r_2}\right| \quad (2)$$

The assumption of a perfect mirror is made, so that R=-1 (the sign minus is due to the fact that the acoustic impedance of air is much smaller than water).

Figure 2 represents maps of SPL_{total} as a function of depth and distance at short range, for S = 1 Pa, d = 4 m and different frequencies. At low frequencies (10 Hz and 100 Hz), because d is much smaller than the wavelength, a dipole-like pattern is obtained as expected. At medium (1000 Hz) and high frequencies (10000 Hz), the interference patterns appear at several slant angles corresponding to a drop in the SPL due to a destructive combination of direct and reflected paths.

Figure 3 shows the SPL plotted as a function of the frequency, for a receiver located at a range of 100 m and 30° slant angle, corresponding to the configuration of Grade C of standard ANSI S12.64. Calculations are performed for 50 frequencies per third-octave bands, for centre frequencies between 10 Hz and 50 kHz. The sound pressure level for an infinite and homogeneous medium (spherical propagation) is plotted with the horizontal black solid line. The narrow band results are plotted in red dotted line, where we obtain a dipole-like behavior at low frequency with a decrease of SPL, and an increasing number of interferences when frequency increases. As the narrowband information is not practical in that case, the standards recommend the use of the third-octave band levels, which are plotted in the black dashed line. The dipole-like is similar as in the narrowband curve, but the high frequency SPL is now approximately 3 dB above SPL_{direct}, instead of 6 dB for the peak values in the narrowband SPL. Besides, ships are not static when measuring their radiated noise. According to the abovementioned standards, the SPL is averaged in a time window corresponding to a +/- 30° bearing angle sector with respects to broadside. This corresponds to the blue line on Figure 3. The difference with the static measurement, i.e. with the ship at CPA (Closest Point of Approach) is very small. For that reason, the following results will only be presented for a static computation with the ship at CPA.

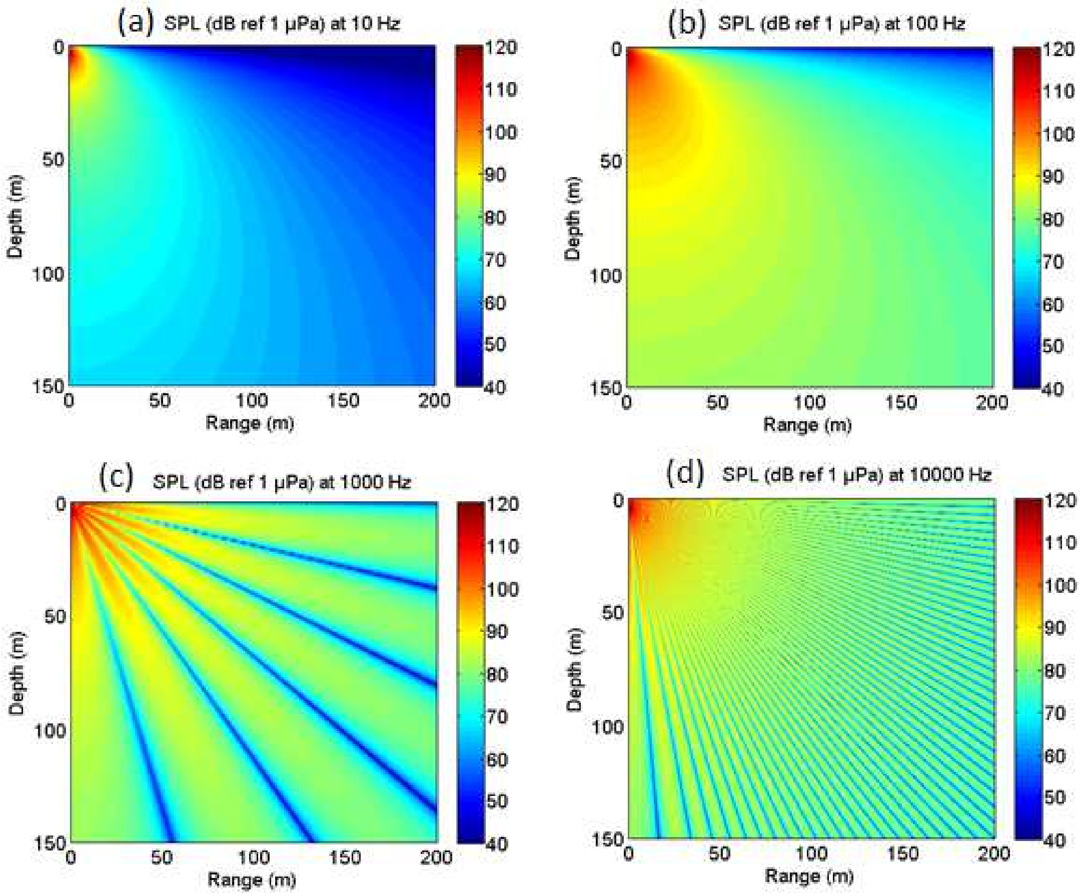

Figure 2: Map of SPL from a point source below sea surface acting as a perfectly reflecting mirror for different frequencies and d = 4 m : (a) 10 Hz, (b) 100 Hz, (c) 1000 Hz and (d) 10000 Hz.

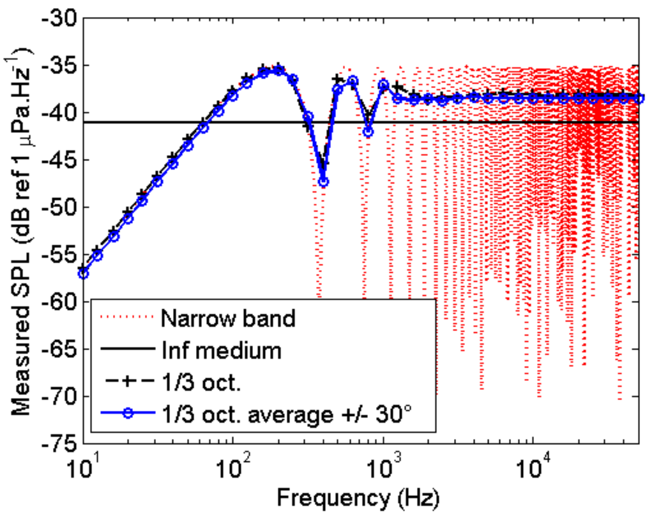

Figure 3: Received level (dB) from a source 4 m below the surface observed at a range of 100 m and a slant angle of 30°.

In order to mitigate the Lloyd's mirror effect and to reduce the uncertainties in the measurement, the ISO standard requires averaging the measurements from 3 hydrophones at different slant angles (15°, 30°, and 45°). The details of the configuration and data processing are given in the standard. On Figure 4 (a), the SPL for the 3 hydrophone locations are presented, superimposed with the spherical spreading result in dotted lines. The phenomena are similar, with however a stronger dipole effect for the 15° angle.

Figure 4 (b) represents the third-octave band averaged SPL with different values of source depth d, for the hydrophone at 30° slant angle. We can note that the curves are the same, but shifted in frequency. As a consequence, in order to estimate the source level S the ISO standardization committee is currently working on a method for correcting the Lloyd's mirror effect.

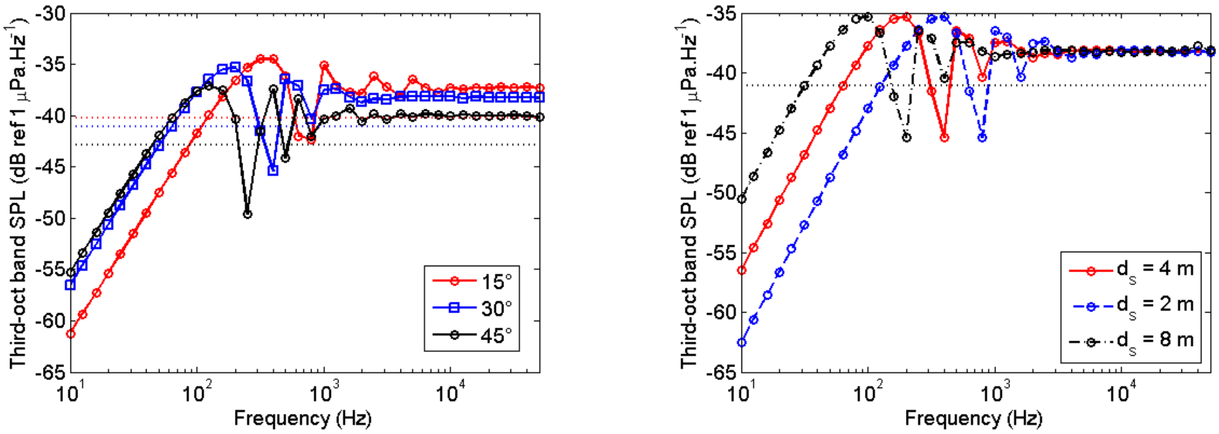

(a) (b)

Figure 4: (a) Measured level (dB) from a unitary source 4 m below the surface for different receiver positions.
(b) Measured level (dB) from a unitary source for different depths for a receiver at 30°.

3 REVIEW OF MODELS FOR THE REFLECTION COEFFICIENT OF A ROUGH SEA SURFACE

Here we are not interested in the scattering (or backscattering) but in the equivalent (or coherent) reflection coefficient, as seen in Figure 5 (figure adapted from Jones (2009)). We can expect that the reflection will be lower if the roughness indicator *h* is comparable or greater than the acoustic wavelength.

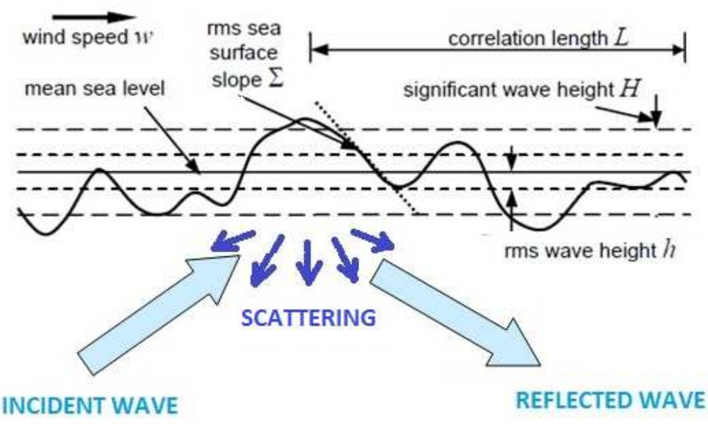

Figure 5: Reflection and scattering of underwater acoustic waves on a rough sea surface.

Below, a literature review of relevant models is presented. Various models of different complexity can be found in the literature, and there are basically three kinds of approaches to tackle this problem:

- Methods based on the Kirchhoff approximation, in a similar manner to those found in optics.
- Perturbation methods used when the RMS surface roughness is small compared to the wavelength.
- Numerical methods.

3.1 Kirchhoff model

The Kirchhoff model is used to describe a sea surface, for instance by Jensen (2000). It is based on the Kirchhoff approximation for scattering, and on the assumption that the sea surface elevation follows a Gaussian probability law of standard deviation *h*, where *h* is the RMS surface roughness. Adding a relationship that links *h* with wind speed *w*, (Jones, 2009) proposes the following formula for the Reflection Loss (RL in dB), where θ has been replaced by sin(θ) to be not only valid for small grazing angles:

$$\mathrm{RL} \approx 8.6 \times 10^{-9} \mathrm{f}^2 \mathrm{w}^4 \sin^2 \theta \qquad (3)$$

3.2 Perturbation methods

The perturbation methods, also known as the Rayleigh-Rice approximation, are widespread approaches to estimate the surface reflection coefficient. Many authors can be cited, for example Harper (1975), Kuperman (1975) and Huang (1998). Nevertheless, the expressions they developed can be heavy to implement and simpler models are presented below.

- Beckmann-Spizzichino model: although it is frequently used, its description is rare in the literature. Jones (2009) writes the Reflection Loss as the sum of a high frequency loss SL_1 and a low frequency loss SL_2:

  $RL = SL_1 + SL_2,$

  $SL_1 = -20\log_{10}(1 - \nu_3)^{1/2}$, where ν_3 is the maximum of $\left[\sin\theta - \frac{e^{-a\theta^2/4}\sin\theta}{\theta\sqrt{\pi a}}\right]$ and $\frac{\sin\theta}{2}$, (4)

  with $a = \frac{1}{2(0.003+5.1\times10^{-3}w)}$ where w is wind speed in m/s and θ is grazing angle in radians.

  $SL_2 = -20\log_{10}\left(0.3 + \frac{0.7}{1+6\times10^{-11}w^4f^2}\right)$

- Kuo's model (Kuo, 1988): Using the Neumann-Pierson wave spectrum to link the RMS wave height *h* with the wind speed *w*, Jones (2009) proposes the following formula for the Reflection Loss:

  $$RL \approx 2.6 \times 10^{-8} f^{\frac{3}{2}} w^4 \sin\theta \qquad (5)$$

- Coherent surface reflection coefficient model: Williams (2004) compares the results of underwater acoustic propagation with different surface reflection coefficients. Besides Kirchhoff and Beckmann-Spizzichino models, they describe a perturbation method in the case of small slope approximation. They point out that the results using Beckman-Spizzichino model show poor results in certain conditions while the small slope approximation performs better. However, the implementation of their method is difficult and the Kirchhoff approximation is sufficient in some cases.

3.3 Numerical methods

A numerical method to estimate the surface reflection coefficient by Thorsos (1990) was first intended to verify the validity of the Kirchhoff approximation. Indeed, many authors suspect the Kirchhoff approximation to not be valid for low grazing angles and for backscattering. Thorsos' approach calculates numerically the solutions of integral equations, taking into account the effects of multiple scattering and shadowing. A Gaussian roughness spectrum describes the sea surface. Monte-Carlo calculations are then performed in order to calculate the Reflection Loss. The results show good agreement in general with the Kirchhoff model, and additional criteria based on the surface correlation length or on the surface slope are proposed to define its validity domain.

In the context of seismic wave propagation, the sea surface reflections at low frequencies (between 10 and 100 Hz) has been studied by Robertsson (2006). The finite difference method and the spectral element method are compared to the Kirchhoff method. The finite difference method solves the first-order partial-differential equations in two space dimensions. The spectral element method is based on the potential form of the wave propagation problem. The main difference with the studies previously cited is that the grazing angles are not small, and that the authors are interested not only in the average power spectrum, but in the actual shape of the response. The authors show that the numerical methods perform very well, but they are limited by their computational costs.

3.4 Comparison of models

We chose to follow a pragmatic approach by using relatively simple models which have an explicit dependence of the reflection coefficient with sea state and/or wind speed. Therefore, we selected three models: Kirchhoff, Kuo's, and Beckmann-Spizzichino. The reflection coefficient in dB is plotted on Figure 6 as a function of frequency for three grazing angles (15°, 30°, and 45°). The wind speed is 5 m/s, which corresponds approximately to sea state 2. Kirchhoff's and Kuo's models perform similarly, with a lower cut-off frequency for the first one. Additionally, the Beckmann-Spizzichino model provides a reflection coefficient dependent on grazing angle at low frequencies.

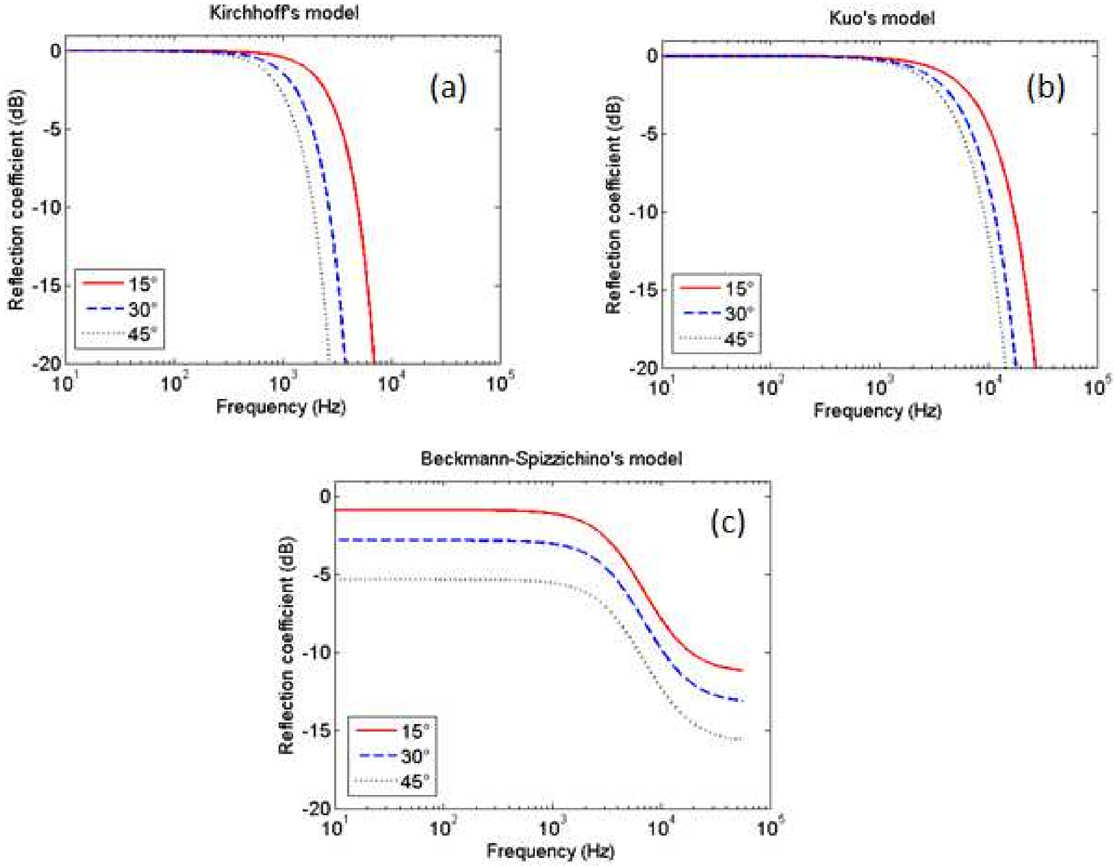

Figure 6: Sea surface reflection coefficient as a function of the frequency for three different models.

The influence of the wind speed for a 30° grazing angle is plotted in Figure 7, using Kuo's model. Not surprisingly, the reflection coefficient is closer to 0 dB (or 1 in amplitude) when wind speed decreases.

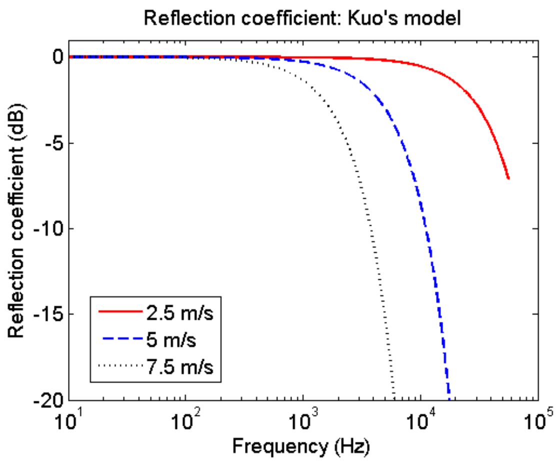

Figure 7: Reflection coefficient for three different wind speeds using Kuo's model.

4 INFLUENCE OF THE REFLECTION COEFFICIENT ON THE LLOYD'S MIRROR EFFECT

Models for reflection coefficient of a rough sea surface are now introduced in eq. (2) giving the total SPL including the Lloyd's mirror effect.

Using the same representation as in Figure 2, Figure 8 shows the maps of SPL of an acoustic source of level 120 dB Re 1µPa located at d = 4 m below sea surface, using Kuo's model for the reflection coefficient of sea surface and a wind speed of 5 m/s. For frequencies 10 Hz, 100 Hz and 1000 Hz, the noise maps are quite similar to the perfect mirror assumption. At higher frequencies, here 10000 Hz, this is no longer the case: the interference patterns disappear and the pressure field is similar to spherical spreading (i.e. a point source in an infinite medium). This is due, at that frequency, to the reduction in the reflection coefficient, as shown on Figure 6 (b).

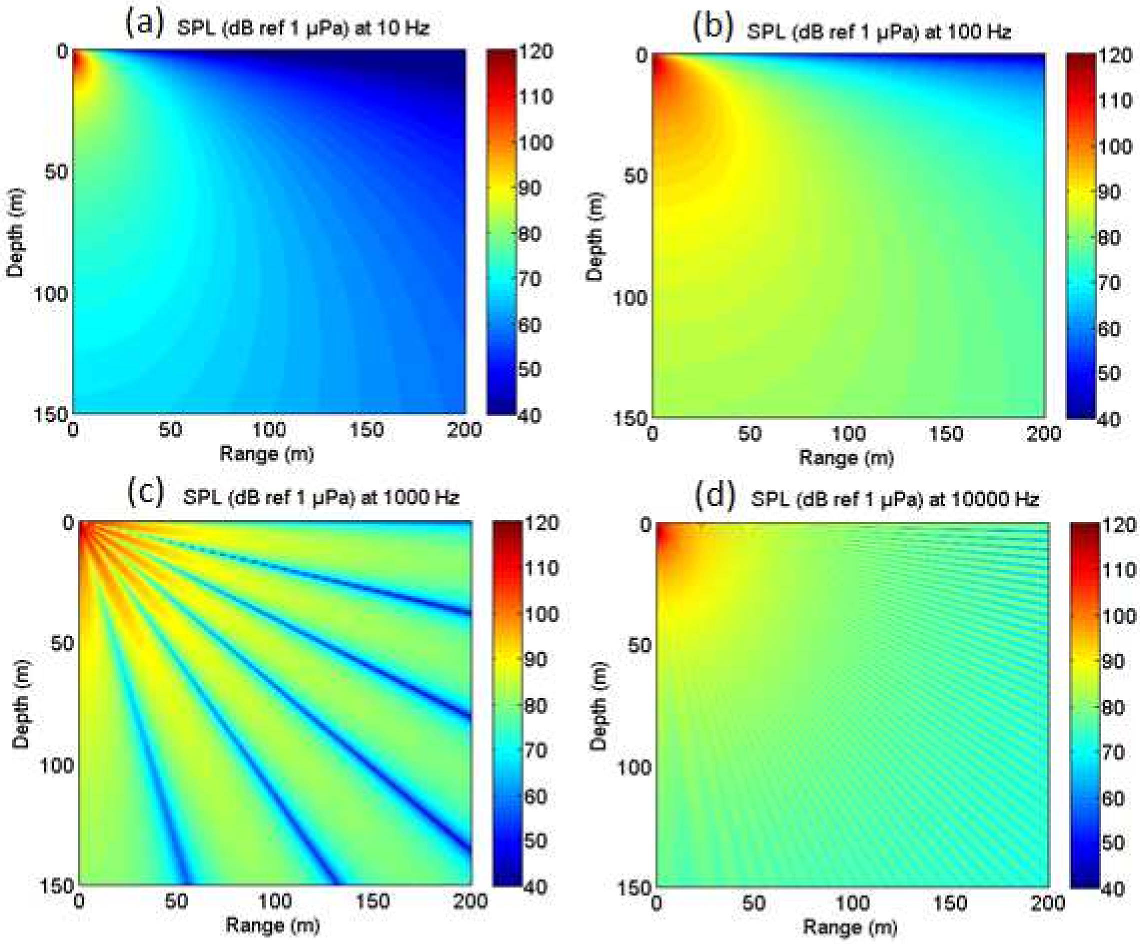

Figure 8: Map of SPL from a point source below a rough sea surface using Kuo's reflection coefficient model for different frequencies and d = 4 m: (a) 10 Hz, (b) 100 Hz, (c) 1000 Hz and (d) 10000 Hz.

Figure 9 shows the results using Beckmann-Spizzichino's model for the reflection coefficient of sea surface with the same input parameters. For frequencies 100 Hz and 1000 Hz, the noise maps are quite similar to the perfect mirror assumption, and at 10000 Hz, the interference patterns disappear in the same way as for Kuo's model. However, there is a difference in the SPL map at very low frequency (10 Hz), as more energy seems to be radiated for large slant angles.

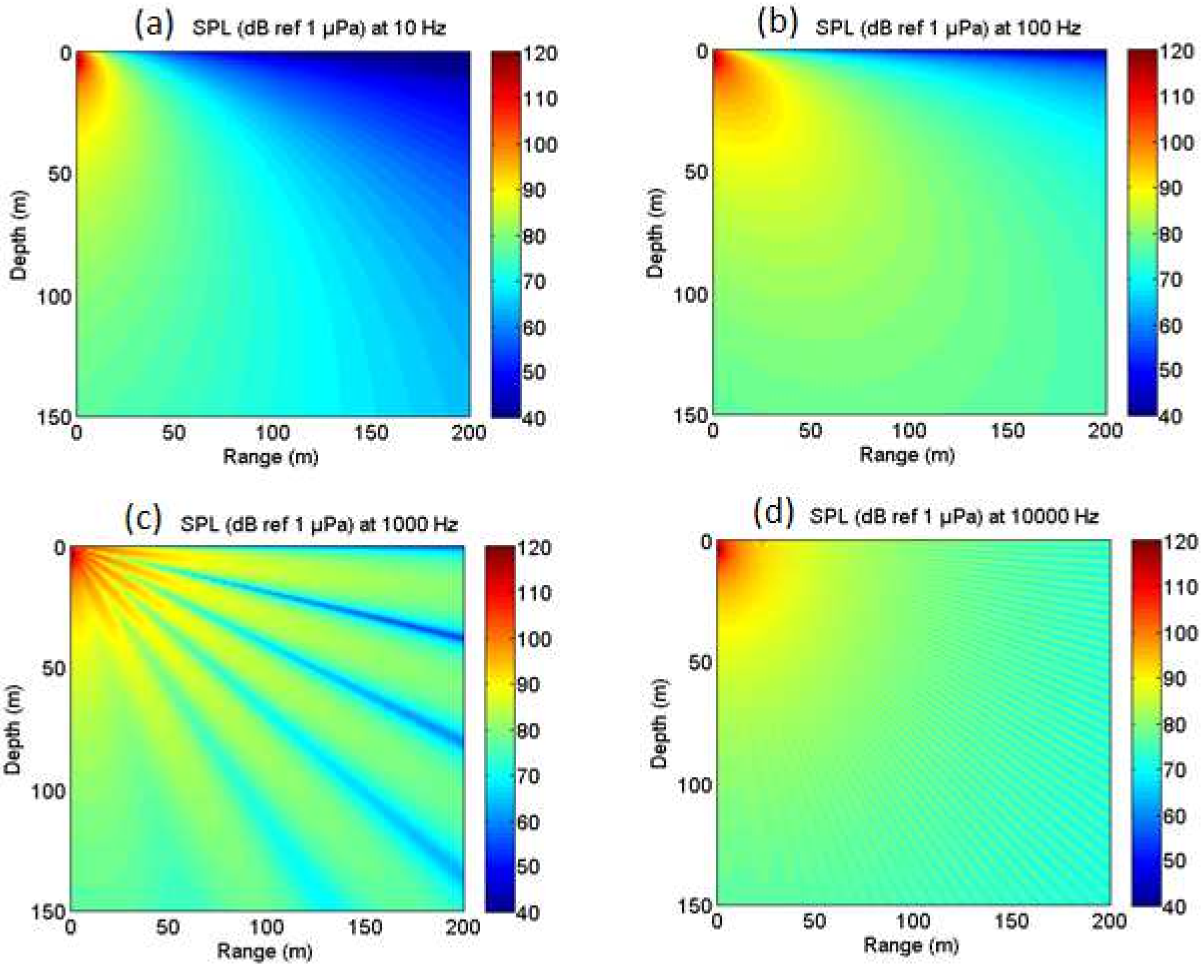

Figure 9: Map of SPL from a point source below a rough sea surface using Beckmann-Spizzichino's reflection coefficient model for different frequencies and d = 4 m: (a) 10 Hz, (b) 100 Hz, (c) 1000 Hz and (d) 10000 Hz.

The frequency responses at the same observation point as for Figure 3 are plotted for different wind speeds and the two reflection coefficient models in Figure 10.

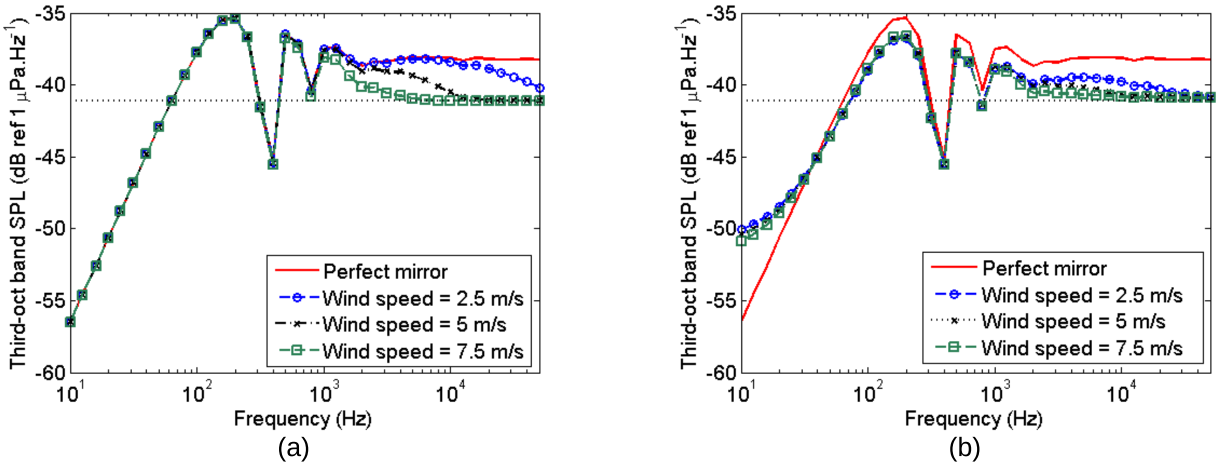

Figure 10: SPL at 100 m distance and 30° slant angle as a function of the frequency for different wind speed using two different reflection coefficient models: (a) Kuo's and (b) Beckmann-Spizzichino's.

With Kuo's model, for the lowest wind speed (2.5 m/s) the curves are close to the perfect mirror assumption up to 10 kHz. When wind speed increases, a 3 dB deviation appears at high frequencies, typically above a few kHz. With Beckmann-Spizzichino's model, we observe that:

- Even with the lowest wind speed, the SPL at medium and high frequencies (above 1 kHz) is lower than with the perfect mirror assumption.
- At very low frequencies, the dependency of SPL with frequency (or angle) doesn't follow exactly a dipole-like behavior, resulting in a deviation exceeding 5 dB at 10 Hz.

5 SUMMARY

With the awareness of increasing underwater noise related to shipping and its impact on marine life, it is of importance to define reliable measurement procedures to determine ship radiated noise, not only for comparison purposes, but in the form of an equivalent sound source level unaffected by boundaries. One of the main phenomena affecting ship radiated noise measurement is Lloyd's mirror effect, related to the interference between the direct sound path and the path reflected on sea surface. After having published a first standard for radiated noise measurement in deep waters for comparison purposes, the ISO committee on underwater acoustics is working on a second part with the objective of correcting the Lloyd's mirror effect. In that context, after a reminder of that phenomenon's basics, the objective of this paper was to outline the effect of the reflection coefficient on sea surface, which cannot be assumed to be a perfect reflector in presence of sea surface waves. A literature review of different models was presented for the acoustic reflection coefficient of sea surface as a function of frequency, grazing angle and wind speed, showing significant differences between them. Further investigation, including comparison with measurement at sea, is needed. Finally, the effect of a non-perfect reflection on the acoustic pressure field emitted by an acoustic source located a few meters below the surface was presented. For all the models, a 3 dB deviation with respects to the perfect reflection assumption is obtained, even at moderate wind speeds. Besides, a particular feature appears at very low frequency if Beckmann-Spizzichino's model is used, with a deviation from the dipole-like behavior. These results should be considered when using procedures for ship radiated noise measurements and correction to the Lloyd's mirror effect. For example, it could lead to under-estimate by 3 dB the ship radiated source level at high frequencies.

6 REFERENCES

Ainslie, M.A., Principles of Sonar Performance Modelling, Springer-Praxis, Chichester, 2010

Audoly, C., Gaggero, T., Baudin, E., Folegot, T., Rizzuto, E., Salinas, R., André, M., Rousset, C.,and Kellett, P., Mitigation of Underwater Radiated Noise Related to Shipping and Its Impact on Marine Life: A Practical Approach Developed in the Scope of AQUO Project, IEEE Journal Of Oceanic Engineering, Vol. 42, N°. 2, April 2017

"Guidelines for the reduction of underwater noise from commercial shipping to address adverse impacts on marine life," IMO MEPC.1/Circ.833, Apr. 2014.

Harper, E. Y. & Labianca, F. M. Scattering of sound from a point source by a rough surface progressing over an isovelocity ocean. The Journal of the Acoustical Society of America, 58(2):349-364, 1975.

Huang, F.-C., Acoustic wave scattering from rough sea surface and seabed – a new look on an old problem. PhD thesis, Institute of Undersea Technology, National Sun Yat-Sen University, 1998.

Jensen, F. B., Kuperman, W. A., Porter, M. B., & Schmidt, H. Computational ocean acoustics. Springer Science & Business Media. 2000.

Jones, A., Sendt, J., Duncan, A., Clarke, P., & Maggi, A. Modelling the acoustic reflection loss at the rough ocean surface. In Proceedings of Acoustics 2009, Annual Conference of the Australian Acoustical Society (pp. 1-8). University of Adelaide. 2009.

Knight, Melanie, Enhancing Cetacean Habitat and Observation (ECHO) Program, EMA BC Workshop, February 2017, http://www.emaofbc.com/2017/02/2017-ema-of-bc-workshop-summary-feb-16-2017/

Kuo, E. Y. Sea surface scattering and propagation loss: review, update, and new predictions. IEEE Journal of Oceanic Engineering, 13(4), 229-234. 1988.

Kuperman, W. A. Coherent component of specular reflection and transmission at a randomly rough two□fluid interface. The Journal of the Acoustical Society of America, 58(2), 365-370. 1975.

Nejedl, V., Stoltenberg, A. and J. Schulz J, Free-field measurements of the radiated and structure borne sound of RV Planet.11th European Conference on Underwater Acoustics, Edinburgh, Scotland, 2-6 July 2012.

Robertsson, J. O. A., Laws, R., Chapman, C., Vilotte, J.-P., & Delavaud, E., Modelling of scattering of seismic waves from a corrugated rough sea surface: a comparison of three methods, Geophys. J. Int., 167, 70-76, 2006.

Thorsos, E. I. Acoustic scattering from a ''Pierson–Moskowitz'' sea surface. The Journal of the Acoustical Society of America, 88(1), 335-349. 1990.

"Underwater noise of research vessels - Review and Recommendations", Cooperative research report, Edited by R. B. Mitson, International Council for the Exploration of the Sea, May 1995.

Underwater acoustics — Quantities and procedures for description and measurement of underwater sound from ships — Part 1: Requirements for precision measurements in deep water used for comparison purposes, ISO 17208-1:2016, International Standardization Organization, Geneva.

Williams, K. L., Thorsos, E. I., & Elam, W. T. Examination of coherent surface reflection coefficient (CSRC) approximations in shallow water propagation. The Journal of the Acoustical Society of America, 116(4), 1975-1984. 2004.